For full citation: https://doi.org/10.1061/JMCEE7.MTENG-15713

Bio-self-healing of cementitious mortar incubated within clay soil

Mohamed Esaker (Ph.D.): Researcher, College of Science and Engineering, University of Derby, Derby DE22 3AW, UK. Email: mohamem.esaker1@unimail.derby.ac.uk

Omar Hamza (Ph.D., CEng.): Senior Lecturer, Division of Civil Engineering, College of Science and Engineering, University of Derby, Derby DE22 3AW, UK. (corresponding author, Email: o.hamza@derby.ac.uk; ORCID: 0000-0002-5048-0423).

David Elliott (Ph.D.): Associate Professor, Division of Microbiology, College of Science and Engineering, University of Derby, Derby DE22 3AW, UK. (ORCID: 0000-0001-9837-7890). Email: d.r.elliott@derby.ac.uk

ABSTRACT

The use of bacteria-based self-healing concrete for sub-structures in ground conditions is an area of increasing interest for enhancing the durability and longevity of infrastructure. In line with this objective, the present study investigates the bio-self-healing performance when a cementitious material is embedded in clay soil with varying chemical exposures and water-saturation regimes. Laboratory experiments were conducted on pre-cracked mortar specimens with *Bacillus Subtilis* encapsulated in perlite. The specimens were then incubated in the soil with different pH and sulphate levels, representing three exposure classes (based on Eurocodes). The crack healing ratio was evaluated through visual inspection and capillary-water absorption - before and after soil incubation. Findings showed that all inoculated specimens exhibited healing ratios noticeably larger than the control specimens, which mainly experienced small autogenous healing. Of note, the best healing performance was observed when the soil was fully-saturated and pH-neutral. From the design perspective of bio-concrete, this study emphasises the consideration of groundwater regime as well as acidity and sulphate of the ground.

Keywords

Bio self-healing; Mortars; Soils and ground conditions; Cracks.

INTRODUCTION

Despite its global popularity as a construction material, reinforced concrete (RC) suffers from micro-cracks, which can increase permeability. This may cause accelerated corrosion of the steel reinforcement (or unwanted leakage issues in the case of concrete reinforced with non-metallic materials), thus leading to early deterioration and shorter service life. The work required to maintain structural performance and restore the durability of concrete can be expensive and time-consuming. To reduce the costly maintenance work, innovative self-healing concretes (Dry 1994; Schlangen and Sangadji 2013; van der Zwaag 2007) have been investigated as a promising solution over the last two decades.

Generally, self-healing in concrete materials can be classified into two major approaches (De Belie et al. 2018; Talaiekhozan et al. 2014; Van Tittelboom and De Belie 2013) - Autogenous and Autonomous. The carbonation of calcium hydroxide ($Ca(OH)_2$) or continuing hydration of clinker minerals (Ter Heide 2005; Yang et al. 2011) means that the natural process of crack healing must be initiated, a process known as autogenous self-healing (Edvardsen 1999). In contrast, the autonomous approach involves the introduction of self-healing agents for more efficient and effective crack healing (Gupta et al. 2018; Yang et al. 2011). Two forms of autonomous healing are developed using: (i) bacterial agents and (ii) chemical agents (Gupta et al. 2018; Mors and Jonkers 2020; Wang et al. 2012). The former method, hereafter termed bio-self-healing, is a solution that is deemed both cost-effective and kind to the environment (Lee and Park 2018; Tziviloglou et al. 2017).

In the bio-self-healing process, robust spore-forming bacteria are used to supplement a concrete mix. To protect these bacteria, they are usually enclosed or prepared with additives such as perlite or alginate. A source of nutrition may also be added to the mix to reactivate bacteria (e.g. Chen et al. 2016). When a crack occurs, allowing moisture to come into contact with the bacteria, a set of chemical reactions will occur in which the bacteria metabolically transform the nutrients (Van Tittelboom et al. 2010); calcium carbonate ($CaCO_3$) is then precipitated.

One of the key elements in bio-self-healing is the provision of a suitable incubation environment to activate the bacteria. Much of the research conducted in this area has examined the healing process of cementitious materials within humid air (Wang et al. 2012), wet-dry cycles (Xu et al. 2013) and various water environments (Palin et al. 2017). These investigated environments are important but may not represent some ambient field conditions, such as the case with sub-structures and tunnels, where concrete is inevitably exposed to different challenging ground conditions e.g. different soil types, groundwater regimes, chemical and bacterial compositions naturally existing within the ground. Understanding the performance of such bio-self-healing concrete is formidably challenged by

the combination of the heterogeneity of micro-crack propagation and the complex physical, hydrological, biological, and chemical properties of the ground. The diverse microbial behaviour of bacteria in response to these conditions adds furthermore to the complexity of this research area. With this complex interaction between the bacteria, concrete, and ground, it is beneficial to understand the influence of environmental factors upon the self-healing process to optimise its performance for field application.

In general, the performance of bio-concrete within ground environments is challenged by various issues (Esaker et al. 2021; Hamza et al. 2020; Souid et al. 2019). These may include the effect of soil bacteria, soil particle infiltration within cracks, pore-water pressure, capillary pressure of cracks, chemical exposures and type of soil. The present study examines the bio-self-healing performance in mortar specimens incubated within clay soil, which complements our previous study conducted within sand soil (Esaker et al. 2021). Clay soils are widely encountered in construction sites and commonly characterised by their fine grains and high water-holding capacities (Hamza and Bellis 2008; Imokawa and Hattori 1985), which can influence the self-healing performance. In this research, varying levels of pH and sulphate that denote industrially established categories of exposure were used to condition and fully/partially saturate the soil. Eurocodes (BSI 2016) were used to select these categories, which classify the risk of chemical attack and corrosion from a hostile ground environment. These classifications range from X0 (no risk) to XA3 (very high risk of aggressive ground). To assess the extent to which cracks had healed, a comparison was made between the amount of water absorbed by the cracks before and after incubation and the area repair rate.

Pursuing this novel research direction is essential due to the ongoing trend of rapid urbanisation, where underground space development is in high demand. Current research on the self-healing of cementitious materials has mainly focused on incubation conditions limited to water and humid air. Our study, by incubating the mortar within clay soil, provides a better understanding of bio-self-healing performance in ground conditions. Aiming to increase the resistance to concrete defects in underground structures, this research area would be of fundamental relevance to concrete scientists and applied relevance to concrete designers.

MATERIALS AND METHODS

Bacteria agents and encapsulation

Cultivation of bacterial strain

The healing agent employed in this research was *Bacillus subtilis* (supplied by Philip Harris, UK). This strain was chosen because previous research indicates it can generate enduring, resistant spores (Kalhori and Bagherpour

2017; Pei et al. 2013). Following Sonenshein et al. (Sonenshein et al. 1974), each strain was grown in Basal medium 121 and its derivatives 121A and 121B. The resulting culture was then incubated in a shaker at 125 rpm at 36°C for 72 h until spores were observed to form. The *stain* method was used to confirm the spore formation under the microscope (LABOPHOT-2, Nikon). To harvest the spores and minimise the presence of vegetative cells, the culture was centrifuged at high speed of 3390 RCF for 10 min and then washed twice using distilled water.

Encapsulation of spores into the perlite

Perlite is commonly used in lightweight concrete and has recently been adopted for bio-self-healing concrete (Alazhari et al. 2018; Zhang et al. 2017). For bio-self-healing concrete, perlite is ideal as it has frequently been applied to lightweight forms of concrete (Alazhari et al. 2018; Zhang et al. 2017). Its extremely porous structure (Fig. 1a), exceeding 20µm, made it an ideal host environment for the healing agent and was thus used to enclose the bacteria and its nutrients. To ensure it conformed with British Standards (BSI 2000), the properties of the perlite were assessed, revealing that it had an open porosity of 65%, unit weight of 128 Kg/m^3 and moisture content of 22%. Moreover, the perlite's particle size distribution (PSD) was examined (Fig. 1b) and indicated that the material was well-graded. Maintaining a consistent particle gradation of perlite is necessary because it may impact the mortar mix and the distribution of bacterial spores, given that perlite serves as a carrier of bacterial spores.

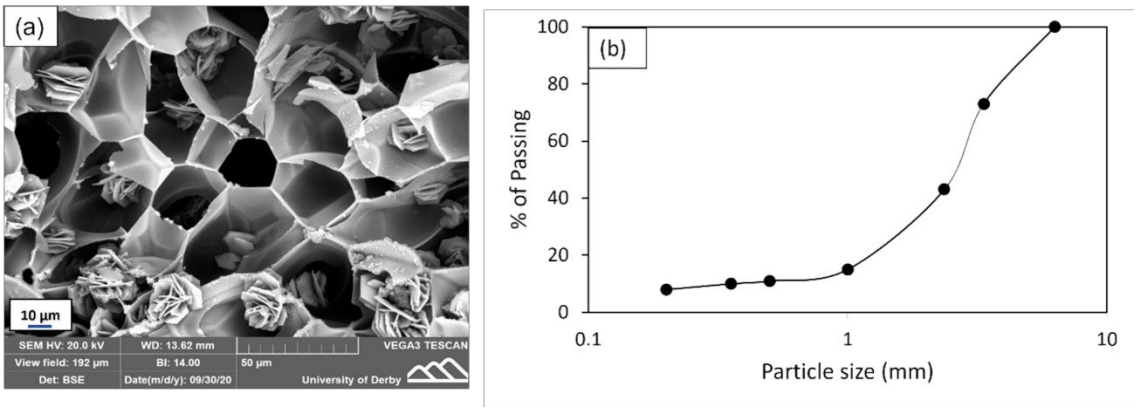

Fig. 1. Properties of perlite: (a) SEM image showing its porous structure, (b) Particle size distribution from Sieve test

To remove moisture and destroy any bacteria or microbes, the perlite was sterilised in the oven for 48 h at a temperature of 160°C. This was followed by immersion in the bacterial suspension for two hours until the latter was completely absorbed. This served to ensure the bacterial spores had fully infused the perlite. A nutrient solution containing yeast extract (6 g/L) and calcium acetate (60 g/L) was sprayed onto its surface (i.e. coating

the outer surface of the particles). The perlite was dried in an oven at a temperature of 40°C for up to 48 h or until its weight remained constant. Around 0.3% of nutrients by perlite weight were contained in each capsule produced. The percentage of nutrients was calculated using the weight of the perlite before and after the infusion, following the procedures outlined in the Microbiology: laboratory manual (Cappuccino and Sherman 2018). The colony Forming Unit (CFU) was then utilised to measure the viability of bacterial spores within the perlite capsules. This revealed that the concentration of viable spores in the perlite capsules was 6.4 x 10^7 CFU/g. Further details on CFU method are provided in the supplementary materials.

Preparation of cement-mortar specimens

Mixtures

Cement-mortar mixtures were prepared to produce Control Mortar Specimens (CMS) and Bio-Mortar Specimens (BMS). The mixtures of both specimens were identical, except that CMS contained no bacteria encapsulated within the perlite. This allows quantifying the effect of bacteria-based self-healing (under different exposure conditions) compared to autogenous healing.

Mix design factors such as water-to-cement ratio can significantly affect the water absorption rate of cement mortar specimens in a test. A higher water-to-cement ratio typically produces a more porous and permeable material with a higher water absorption rate. This is because excess water creates voids and capillaries in the hardened cement paste, which can act as channels for water to flow through. Therefore, the mixture was carefully controlled in this study and followed the procedures recommended in BS EN 480-13:2015 (BSI 2015) to maintain consistency across all mortar specimens. This was accomplished by mixing Hanson Sulphate Resisting Cement (CEM III/A +SR), sand, tap water, and perlite impregnated with a self-healing agent. The proportions of both mixtures (BMS and CMC) are given in Table 1, where the water-to-cement ratio was 0.5.

Table 1. Proportion of the mixture used for the control (CMS) and bio mortar specimens (BMS)

Ingredient (Kg/m^3)	Mixture	
	Control (CMS)	**Bio-Mortar (BMS)**
Cement	450	450
Sand	761	761
Water	225	225
Perlite (with Bacteria & Nutrients)	-	22.5
Perlite (without Bacteria & Nutrients)	22.5	-

Casting

The mortar mixtures were cast into metal moulds to produce two specimen geometries: discs and prisms. In total,

fourty-eight specimens were produced, including three prismatic and three disc-shaped specimens for each of the four exposure classes/soil conditions, as described in the following sections.

The disc-shaped specimens (with a height of 40 mm and a diameter of 100 mm) were employed to visually inspect the crack sealing. We chose this shape for the visual inspection of cracks due to its advantages, including the ability to generate more cracks from both sides of the specimens.

However, visual inspection is limited to surface-level information on the precipitation sealing the cracks, and to assess the self-healing inside the cracks, water absorption testing was conducted. This method has been widely used to evaluate the restored transport properties (Gardner et al. 2014). The prismatic specimens (measuring 40 x 40 x 160 mm) were selected for the water absorption testing.

It was important to prevent total failure when the cracks were propagating; therefore, the prisms were strengthened during casting using a fibre mesh positioned at each specimen's centre. Once 24 h had passed, the mortar specimens were taken from the moulds and stored in water for 28 days to cure them. At the end of this curing period, the specimens were removed and dried at room temperature, following which standard mechanical testing was employed to generate the cracks.

Cracks generation

Cracks were generated in the specimens (prisms and discs) using mechanical testing. A splitting test was used for the discs and a three-point bending test for the prisms. The prism was placed on two parallel beams located on the bottom side. The distance separating these beams was roughly two-thirds of the total length of each specimen. Linear Variable Differential Transducers (LVDT) were secured to the bottom of the specimen to control the cracks that were induced. Gradual application of the load at a velocity of 0.001 mm s^{-1} then took place until a crack formed. The velocity was then gently reduced so that the crack formed around the specimen without resulting in its failure. The specimen was then unloaded, causing a reduction in crack width. No full failure was observed during this stage as fibre meshes centrally reinforced the prismatic specimens.

Carbon fibre adhesive tape was used to wrap the cylindrical specimens to prevent collapse as the cracks formed under indirect tensile stresses. During the splitting test, the specimen was positioned horizontally between the bottom and upper plates in the uniaxial compressive strength test machine. The load was then applied at an extremely low speed until a crack could be seen on both sides of the discs, at which point loading was terminated. Multiple cracks were observed through this process, ranging from 60µm to 350µm in width. Shuttlepix Editor software was utilised to take regular measurements of these cracks; this was essential to ensure a comparable range of crack widths in each incubation environment.

Preparation of soil for incubating the pre-cracked mortar specimens

Soil classification tests

The pre-cracked cement-mortar specimens were incubated in clay, which is cohesive, plastic and fine-grained soil. This type of soil was considered for the experiment because it is widely encountered in construction sites in the UK (Bell and Jermy 1994) and many other regions worldwide.

In this work, the soil was sourced from Pot-Clays (UK) - mainly containing clay with some silt. The clay content comprises kaolinite, which has been widely used in fundamental studies in geotechnical engineering (Hamza and Ikin 2020). The soil was tested to characterise its physical properties, including plasticity and grading, according to British Standards (BSI 1990a). The particle size distribution (PSD) of the soil mixture was 100% smaller than 63μm, including 68% pure clay (< 2μm) and 32% Silt. The Plasticity and Liquid Limits are 24% and 45%, respectively, indicating that the silty clay has intermediate plasticity.

Soil saturation regimes

Clay soils are generally water-sensitive where pore-water pressure (u) significantly depends on the variation of moisture content and degree of saturation. For instance, when the clay is fully saturated, the (u) value is positive but can become negative (suction) in a partially saturated condition. The soil needed to be in a fully saturated condition (FSC) for most of the tests. This meant it was essential to determine the minimum moisture content at which the pressure of the pore-water was within standard 'equilibrium' values ($u = 0$) or was positive. This entailed examining soil suction at different levels of moisture content. A miniature tensiometer (UMS T5 by Labcell LTD) connected to a compatible data logger was used to measure the soil suction. Fig. 2 presents a plot of the suction and moisture content, which provides a reasonable approximation of the soil-water characteristics curve (Gonzalez-Ollauri and Mickovski 2017). This shows that the suction increases with soil dehydration and is principally dependent on the moisture content. Accordingly, the following moisture contents, 48% and 25%, were considered for the fully and partially saturated conditions (FSC and PSC), respectively. For both conditions, we had also to control the densities as this can influence the saturation. Fig. 2 also summarises these soil parameters considered in both conditions (FSC and PSC), including moisture, suction and density.

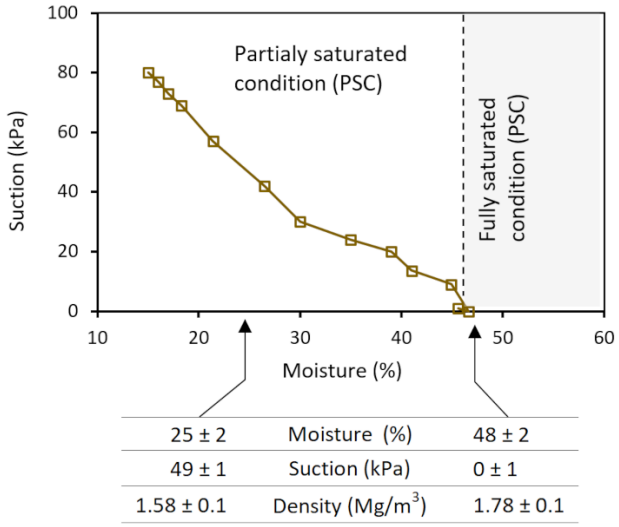

Fig. 2. The relationship between the measured suction and average moisture content of the soil. The moisture contents of 25% and 48% were considered for the partially and fully saturated conditions, respectively

Chemical conditioning of the soil

The soil was conditioned to represent two hydrological regimes, including fully and partially saturated conditions (FSC and PSC, respectively). To represent three exposure classes (X0, XA1 and XA3) in line with BS EN 206:2013+A1:2016 (BSI 2016), three hostile environments were prepared for FSC. As explained previously, these classes denote the risk of chemical attack and corrosion from an aggressive ground environment. Class X0 was the control class, with a neutral pH of approximately 7, whereas classes XA1 and XA3 had their pH values altered to around 6 (moderately acidic) and 4.5 (very acidic), respectively. Only class X0 was considered for the PSC.

The sulphate salt found most often in the ground is calcium sulphate (BSI 1990b). Therefore, the soil pH was adjusted to the required level by mixing the soil (and any added water) with calcium sulphate (supplied by Sigma-Aldrich Ltd, UK) in the percentages shown in Table 2. This was confirmed by measuring the soil pH using a portable meter.

Table 2. Limiting values of calcium sulphate used to achieve the desired exposure classes

Exposure class	**X0**	**XA1**	**XA3**
Calcium sulphate (mg/Kg)	0	≥ 2000 and ≤ 3000	>12000 and ≤ 24000
pH range	≥ 7 and < 7.4	≥ 5.5 and ≤ 6.5	≥ 4 and < 4.5
Achieved pH	7.2 ± 0.2	5.9 ± 0.2	4.3 ± 0.2

Incubating the specimens within soil

Immediately after the inspection of the cracks (as described in the next section), the specimens were wrapped with

light cloth around the cracked area to prevent the clay particles from being trapped within the cracks. Six mortar specimens were incubated for each exposure class for 120 days within the clay, prepared in advance according to properties specified in Tables 1 and 2. Plastic boxes (350 x 600 x 400 mm) were used for the incubation, with 300mm soil thickness. The soil was prepared in a workable slurry (slump) with the required moisture content and lightly compacted in layers where the first layer reached 100 mm from the bottom before placing the mortar specimens. Then, the second layer was carefully placed around the specimens creating a thickness of 200mm.

During the soil incubation, CMS, which are not inoculated with bacteria, were separated from the BMS and incubated in separate soil boxes to avoid any potential cross-contamination, i.e. immigration of spores and nutrients from the crack zone through the soil pore water.

EVALUATION OF CRACK HEALING EFFICIENCY

Visual inspection and image analysis

Using a digital microscope (Nikon P-400R, Japan), the cracked specimens were visually examined before and after soil incubation to assess the healing ratio. Once each crack had been generated, it was marked in 3 to 4 places in a uniform fashion along its length. Before and after incubation, photos of these cracks were taken. Prior to the inspection, the soil was subjected to ultrasonic cleaning (within the water) after incubation to ensure any residual soil particles were removed. For each photo, *ShuttlePix Editor* Software (Nikon, Japan) was used to measure the width of the crack at each position close to the markers. Using open-source software ImageJ, an additional analysis of the images was then performed to assess the healing ratio for each specimen (Schneider et al. 2012). ImageJ provides a measure of areas and distances and can generate density histograms.

Consequently, an estimate was provided of the extent to which the area fraction of each crack had decreased. This was represented by black pixels that denote the cracks in a microscopic image following incubation. Overall, 72 microscopic images were gathered along the lengths of the cracks for each type of specimen and analysed using ImageJ. The average (mean) healing ratio was then calculated using Equation 1.

$$\textit{Average healing ratio} = \frac{1}{\mathrm{n}}\sum_{1}^{n}\frac{A_i - A_f}{A_i} \qquad (1)$$

Where:

A_i = the initial area of crack

A_f = the final area of crack

n = the total number of locations of the cracks analysed

Capillary water absorption test

Visual inspection alone yields information mainly about the surface sealing of the crack through precipitation, prompting us to supplement our approach with the water absorption test to obtain a more comprehensive understanding of self-healing within the crack's interior. Our focus was primarily on the restoration of transport properties, and thus we did not perform strength testing. It is worth noting that other researchers have reported restored strength in cracks that have been sealed.

Following standardised procedures, capillary water absorption was used to assess the healing efficiency (ratio) (BSI 2004). This non-destructive test associated with crack tightness can be employed to measure the water tightness of the specimens at any crack-sealing stage (Gardner et al. 2014). Capillary suction is caused by unequal surface tension between the fluid-solid and fluid-fluid interfaces (Martys and Ferraris 1997). Thus, the sorption coefficient (S) before and after soil incubation was calculated by measuring the water absorption rate in the capillary suction of the oven-dried mortar specimens.

For at least seven days, the prismatic mortar specimens were oven-dried at a temperature of 40°C until a change in mass of less than 0.2% in 2 hours was observed (Gardner et al. 2014). Before beginning the test, the sides of each prism were coated with epoxy resin to ensure they were resistant to water. Apart from a small 20 mm x 40 mm area around the crack, epoxy resin was also used to coat the bottom surface. This specific coating method was implemented to restrict water absorption to the crack areas on the specimen's surface. Initial recordings were made of the initial weight of each specimen. The test faces of all specimens were then positioned on two plastic strips in a tray with a loose lid to ensure air could not move around the specimens. As indicated in Fig. 3, distilled water was poured into the tray to a depth of between 2.0 ± 0.8 mm above the level of the plastic strips.

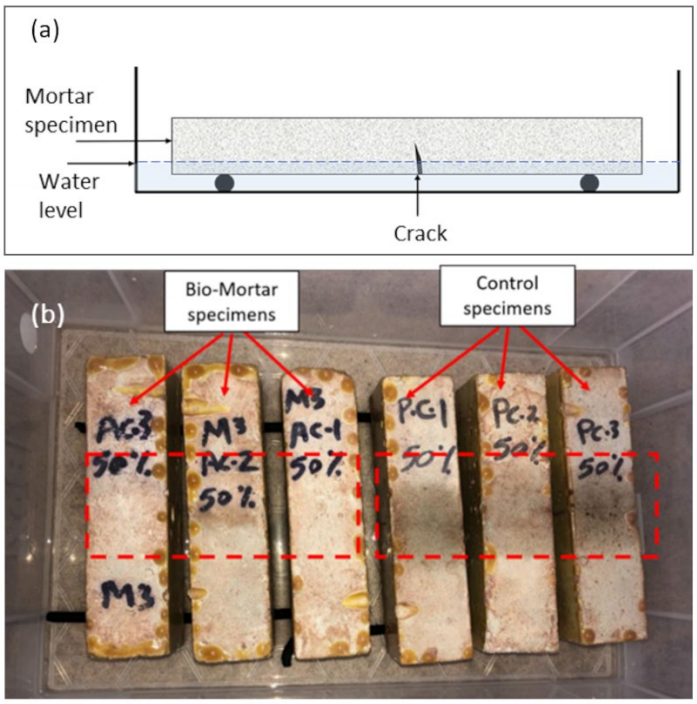

Fig. 3. (a) Schematic illustration of capillary water absorption test set-up; (b) Water uptake during one of the tests conducted for the control and bio-mortar specimens after soil incubation

An electronic balance accurate to 0.01g then measured the change in the water absorption rate of the BMS and CMS before and after incubation. Before weighing, a damp cloth was used to wipe the specimens to remove any surface water. Water uptake was measured after 12 min, 30 min, 1 h, 2 h, 3 h, 4 h, and 6 h. The following equations were then used to calculate the absorption and sorptivity coefficients (*I* and *S*) (BSI 2004):

$$I = \frac{m_t}{a.d} \quad (2)$$

$$S = \frac{I}{\sqrt{t}} \quad (3)$$

Where:

I = coefficient of absorption

m_t = change in specimen mass in grams at time t

a = exposed area of the specimen in mm^2

d = density of the water in $g.mm^{-3}$

S = coefficient of Sorption ($mm/\sqrt{s}$)

The healing percentage was calculated according to the following equation:

$$Healing\ ratio = \frac{(S_i - S_f)}{S_i}\ x\ 100 \quad (4)$$

where S_i and S_f are coefficients of Sorption before and after incubation, respectively.

Characterisation of healing production using SEM and EDX

Microstructure analysis can help characterise the healing products by visualizing and quantifying the healing products' size, shape, and distribution, as well as their interaction with the cementitious matrix and the crack surfaces. In this study, following the visual inspection and water absorption testing, a Scanning Electron Microscope (SEM) and energy-dispersive X-ray spectroscopy (EDX) were employed to determine the chemical compositions and crystalline structure of the self-healing products for the BMS and CMS.

Initially, the specimens were left to stand for two days at room temperature until they were totally dry. To fit the chamber of the SEM machine and limit the porous effect during coating, they were sliced into tiny pieces (10 x 10 mm) around the healed crack. The sample was then fixed for 10 min by placing the specimens in a cylindrical disc chamber containing several holes. This enabled the formation of a conductive layer of gold on the surface of the specimen, which was created by the low vacuum coating of the sample. To allow an image to form one pixel at a time, an electron beam was applied in a raster fashion across the sample's surface using 20 KV voltage.

RESULTS AND DISCUSSION

Visual evaluation of crack and healing quantification

After soil incubation, CMS and BMS specimens were first removed from the soil (their incubation environments) and then immersed in water for ultrasound cleaning before being visually inspected under the microscope to evaluate the crack closure. Fig. 4a shows typical top views of the crack surface of the maximum healed crack widths of bio-mortar specimens before and after the incubation in four different exposure conditions (FSC-X0, FSC-XA1, FSC-XA3, and PSC-X0). As shown, the widths of completely healed cracks were relatively larger in specimens incubated in fully saturated, pH-neutral soil (FSC-X0) (250μm) than the specimens incubated in FSC-XA1 and FSC-XA3 (220 and 189 μm, respectively). For bio-mortar specimens incubated in partially saturated pH-neutral soil (PSC-X0), only a few locations were completely healed, and the maximum healed crack width was around 170 μm. It was also noted that a thin and discontinued layer of calcium carbonate crystals was formed at the top of the cracks.

The microscopic inspection of the CMS – in Fig. 4b - showed that the crack was more difficult to repair autogenously with the increase in average crack width. Based on the microscopic inspection (Fig. 4.b), the autogenous healing due to the late hydration of un-hydrated cement particles was effective for average crack width of 60–120 μm, where most cracks within this range healed. It is important to note that these findings were drawn

from the images obtained from all cracks, reflecting an overall change in crack width. The analysis of all cracks ensures that the results represent the material's overall behaviour instead of being influenced by a subset of cracks, thus minimizing any potential bias.

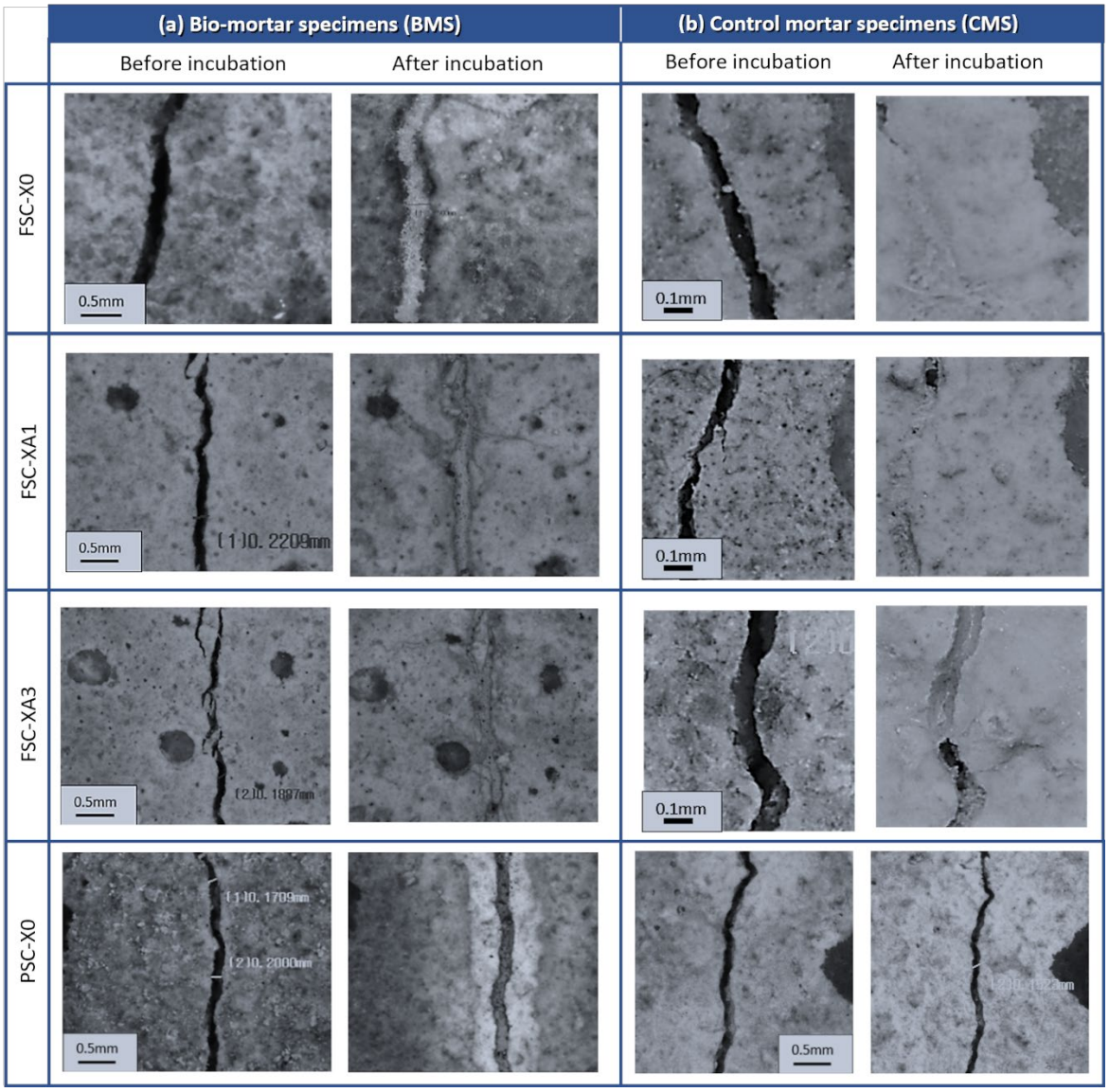

Fig. 4. Microscopic observation of crack healing of specimens (BMS and CMS) before and after incubation in fully and partially saturated clay (FSC and PSC, respectively)

To quantify the healing ratio, the images of the cracks before and after incubation were processed to obtain the crack area using “image J” software. Based on this microscopic visual inspection and image analysis, Fig. 5a presents the average (mean) crack healing ratio of the control and bio-mortar specimens incubated in different exposure classes. The error bar (with the upper and lower values) is added to the figure to indicate the variability in the reported measurement.

As Fig. 5a shows, the healing ratios for all BMS are almost two-fold the healing ratios of control mortar CMS for

all exposure classes. This explains the white crystalline precipitation of calcium carbonate induced by bacterial metabolic conversion of nutrients (Perito and Mastromei 2011), as suggested by the EDX analysis (as presented in the next section).

It was also indicated that the soil pH slightly influenced the healing performance of bio-mortar specimens. For instance, the healing percentage of bio-mortar specimens incubated in FSC-XA3 was around 7% lower than in the specimens incubated in FSC-X0. The lower pH value in the soil environment can be linked to the decline in the healing capability of BMS incubated in XA1 and XA3. This is supported by a previous study conducted by Knoll (Knoll 2003), which found that a high pH favours the formation of carbonates from bicarbonates. However, the repairability of the microbial agent was more noticeably limited in the specimens incubated within the partially saturated condition (PSC-X0), where the corresponding healing ratio was approximately 38%.

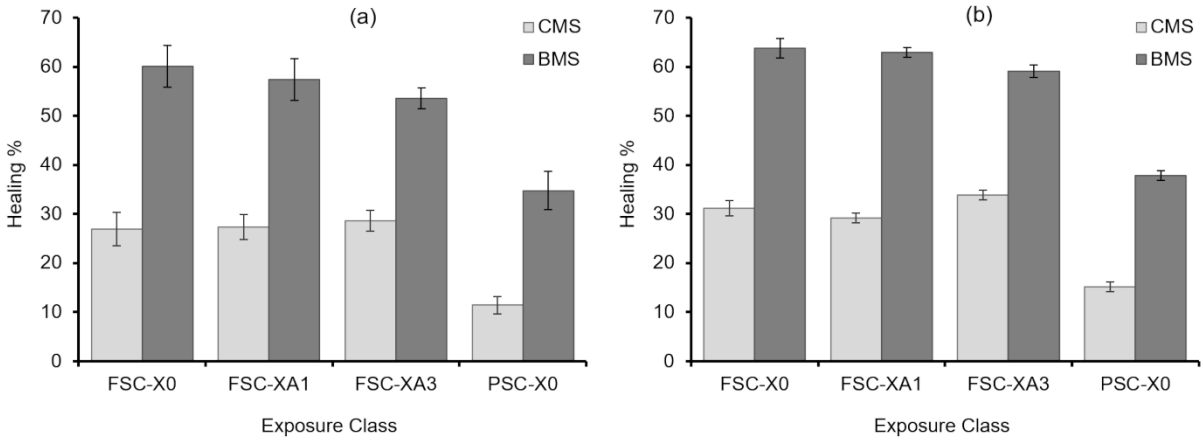

Fig. 5 The average (mean) healing percentages of BMS and CMS based on: (a) macroscopic visual inspection (b) change in water absorption rate (before and after soil incubation under varying exposure conditions)

Looking at the healing percentage of the control mortar specimens (which did not have any bio-healing agent), it is evident that the healing ratio was low and relatively similar in the three different exposure classes (31%, 29%, and 33% for FSC-X0, FSC-XA1, and FSC-XA3, respectively) – despite these were all incubated in fully saturated condition FSC. However, the healing percentage of the control mortar specimens incubated in PSC-X0 was noticeably lower (15%) than in specimens incubated in FSC. The autogenous healing of cementitious materials has a certain capacity, and this capacity is mainly affected by the composition of the matrix and the environmental exposure conditions. In FSC exposure class, the hydration of the un-hydrated cement particles and swelling of the hydration products were more effective than in PSC due to the presence of water.

Water absorption results

Fig. 6 shows the change in capillary water absorption of the cracks before and after the soil incubation. The results

indicate that the sorptivity coefficient for all specimens (CMS and BMS) decreased after incubation due to crack healing. Based on the percentage change in the sorptivity coefficient (S), the average healing ratio was calculated and plotted in Fig. 5b. For the BMS incubated in fully saturated clay (FSC), a relatively lower water absorption rate was obtained for exposure class X0, where the healing ratio was around 59.5% in comparison with specimens incubated in other exposure classes XA1, and XA3 (57.1% and 53.6%, respectively).

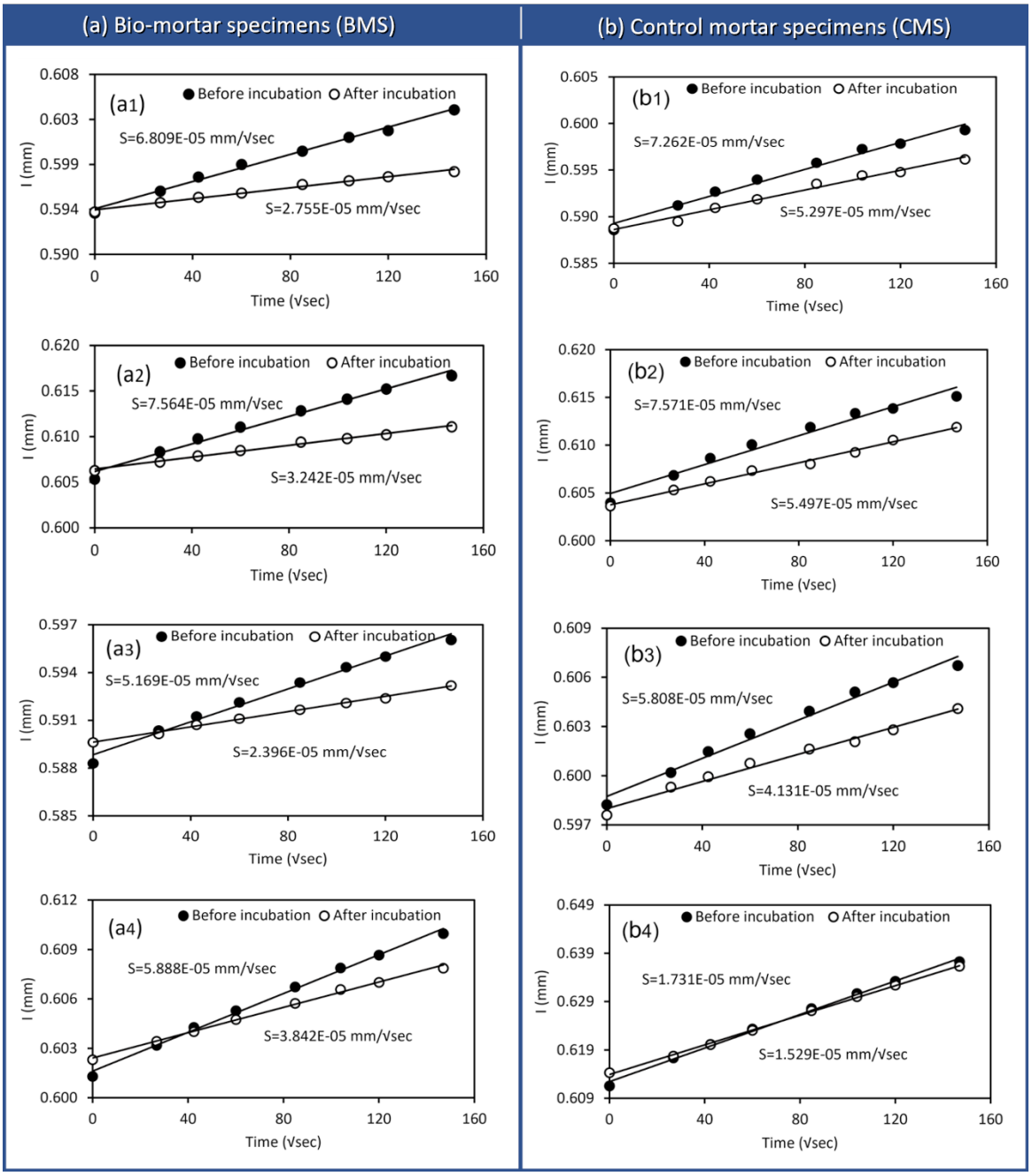

Fig. 6 Change in capillary water absorption of (a) the bio-mortar specimens (BMS) and (b) control mortar specimens (CMS) before and after incubation in different environmental exposure conditions: (1) FSC-X0, (2) FSC-XA1, (3) FSC-XA3, and (4) PSC-X0. (Note. The corresponding healing ratio is plotted in Fig. 5b)

The results (Fig. 5b) also reveal that the healing ratio of the bio-mortar specimens incubated in partially saturated clay (PSC) exhibited a smaller reduction in absorption rate compared to that of identical specimens incubated in fully saturated clay (FSC). For instance, the healing ratio of the specimens incubated in X0-PSC was around 34%, whereas that of specimens with a similar exposure class incubated in FSC was 59.5%. According to the concept of bio-self-healing concrete (Jonkers and Schlangen 2007), one of the main factors is that enough self-healing agents should be transported to the crack surface and activated by water contact. For the fully saturated condition (where moisture content = 47%), all the pore space is filled with liquid and no matric suction in the soil (i.e. according to the Tensiometer measurement, Fig. 1). Therefore, the bacteria would be exposed to the crack surfaces and activated as soon as they became in contact with water ingress from the surrounding fully saturated soil. Then, the precipitations of calcium carbonate form due to the equilibrium between Ca^{2+} and CO_2 with $CaCO_3$ (Eq. 5) (Thomas et al. 2014).

$$Ca^{2+} + H_2O + CO_2 \leftrightarrow CaCO_3 + 2H^+ \qquad (5)$$

In contrast, for the partially saturated condition (PSC), a layer of moisture covering the soil particles and a menisci shape layer at the contact points with the cracked specimens were formed as a result of the capillary and adsorptive forces (suction), whereas the rest of the pore space was occupied by air. In such conditions, the clay soil attracts water molecules that become less available in the cracks leading to the lack of necessary conditions for the self-healing process. This implies that self-healing performance is significantly affected by the moisture content of the clay soil.

On the other hand, the pre-cracked CMS (without any added bacteria) were autogenously healed, and the healing percentages for specimens incubated in FSC are generally similar (27.1%, 27.4%, and 28.9%) in all the exposure classes (X0, XA1 and XA3 respectively). However, in all relevant reaction processes for autogenous healing, like secondary hydration of un-hydrated cement particles and swelling of hydration products, water is the key element to proceed with such reactions. Therefore, all these reactions would be significantly influenced or not happen without the presence of water. Thus, the healing percentage of the CMS incubated in the partially saturated condition (PSC-X0) was relatively lower (11.7%) in comparison with the healing percentage of specimens incubated in FSC-X0 and identical exposure class (27.1%).

In summary, there was a decrease in the absorption rate of bio-mortar specimens in comparison with the control specimens in all environmental exposure classes (e.g. Fig. 5b). The reduced permeation properties are associated with the deposition of crystals of calcium carbonate on the crack surface as evident from the SEM images (see

next section). As demonstrated in Fig 5, the mean values of the healing ratios obtained from water absorption tests are similar to those obtained from visual inspection, despite the differing upper and lower error values between the two methods.

In comparison with a previous study (Esaker et al. 2021) conducted by the authors on identical mortar specimens but incubated in different soil (i.e. sand) and subjected to fully and partially saturated cycles for 120 days, the self-healing ratios were generally larger by about 11% and more sensitive to the variation of pH level than the current study. This might be attributed to the pore permeability of the clay soil used in this study, which would restrict the movement of water around the crack and eventually slow down the production of calcium carbonate and reduce the effect of pH (from the water). However, further research is required as biological features and other abiotic factors likely influence these results. For example, the capacity of microbes to produce CO_2 might be restricted by the existence of a soil matrix that prevents oxygen and other resources from being transported to them.

Microstructure analysis of healing products

Samples from the precipitated materials on the crack surface (after the incubation) were examined by SEM to configure the shape of the crystals. To determine the chemical composition, the samples were further subjected to EDX analysis, which was conducted on a point with pixel size ranges between 6250 to 8435 and an acceleration voltage of 20KV. The SEM images and EDX analyses for the bio and control mortar specimens are shown in Figures 7 and 8, respectively.

From Fig. 7 (a, b, and c), the SEM images revealed that the crystals (of calcium carbonate) in the bio-mortar specimens exhibited a granular blocky and laminar close packing morphology, which were attached to the crack walls and might have served as a front line for resisting water penetration (as observed in the water absorption tests). The blocky and granular morphology suggests that the crystals are growing in a relatively uniform manner, forming compact and densely packed clusters. The laminar morphology suggests that the crystals are forming thin, sheet-like structures that are arranged in layers. This type of crystal morphology can be advantageous for enhancing the mechanical properties of the healed region by providing a more effective bonding between the crack surfaces.

The EDX result (Fig. 7d, e, and f) of the bio-mortar specimens samples revealed that the precipitation at the surface of the cracks was essentially an association of oxygen, carbon, and calcium atoms, suggesting the presence of calcium carbonate. These observations are in agreement with previous studies that have reported the precipitation of calcite and ettringite as the major healing products in the bio-self-healing of cementitious materials

(Gupta et al. 2018; Jonkers and Schlangen 2007).

For the control specimens, on the other hand, the SEM images of the healing products in Fig. 8 (a, b, and c) showed discrete crystals of ettringite and calcium hydroxide – most likely generated by the reaction between calcium aluminate in the cement and sulphate compounds. These crystals were also attached to the crack walls, forming a partial barrier to water absorption. The formation of ettringite and calcium hydroxide crystals is a common mechanism for autogenous self-healing in cementitious materials, including mortars. Ettringite is a calcium-aluminium-sulphate-hydrate mineral that forms as a result of the reaction between the calcium aluminate in the cement and sulphate compounds, such as gypsum or anhydrite. Calcium hydroxide, also known as portlandite, is another hydration product of cement that can form during the autogenous self-healing process (Alghamri et al. 2016). The presence of Ca, Si, and O was indicated by the EDX analysis of the healing product (Fig. 8d, e, and f). This is because the ongoing hydration of unhydrated cement particles led to the creation of calcium silicate hydrate (C-S-H).

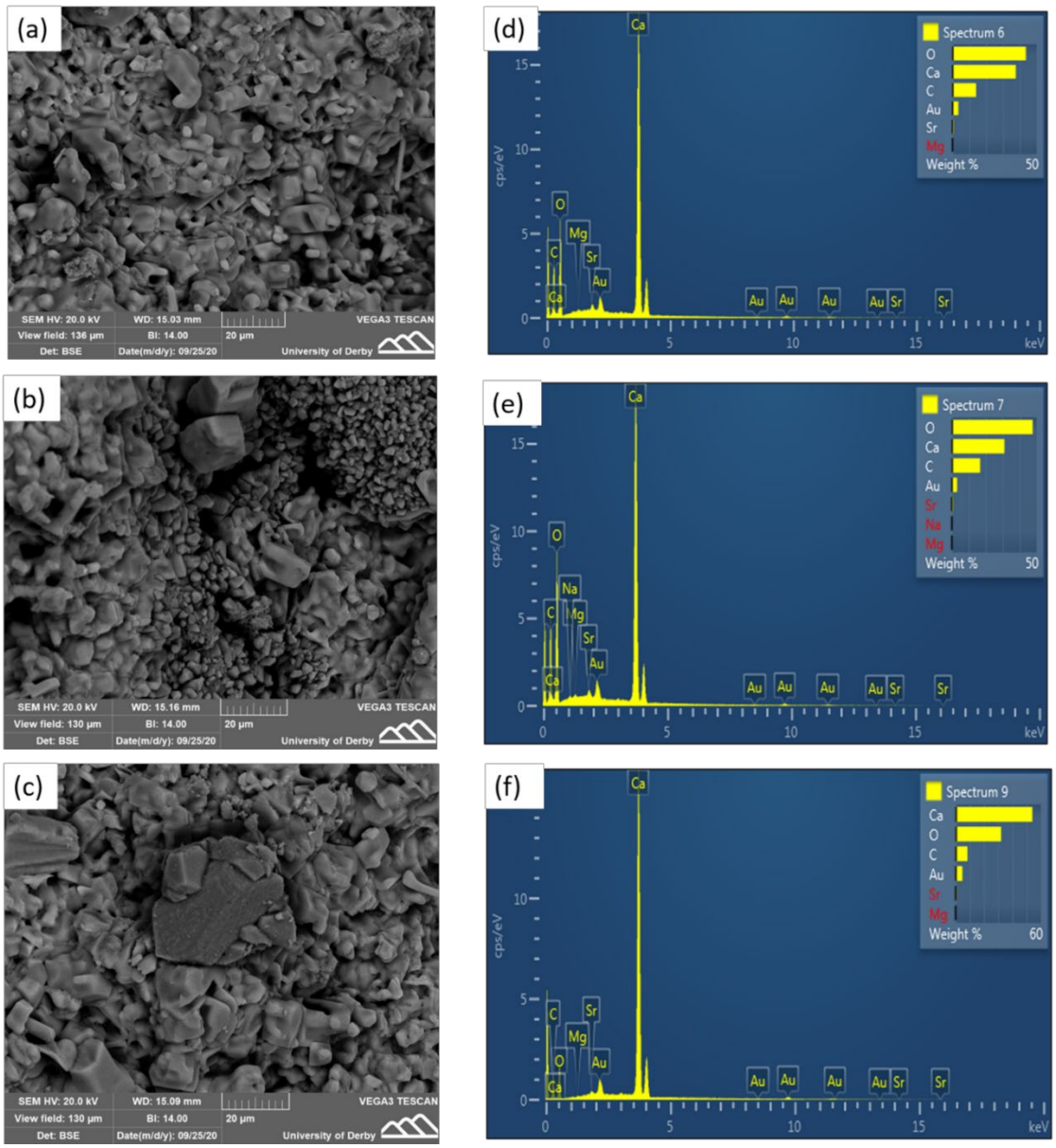

Fig. 7 (a, b, and c) SEM images of the healing products of the bio-mortar specimens BMS incubated in X0, XA1, and XA3, respectively. (d, e, and f) EDX analysis of the healing products of the bio mortar specimens incubated in X0, XA1, and XA3, respectively

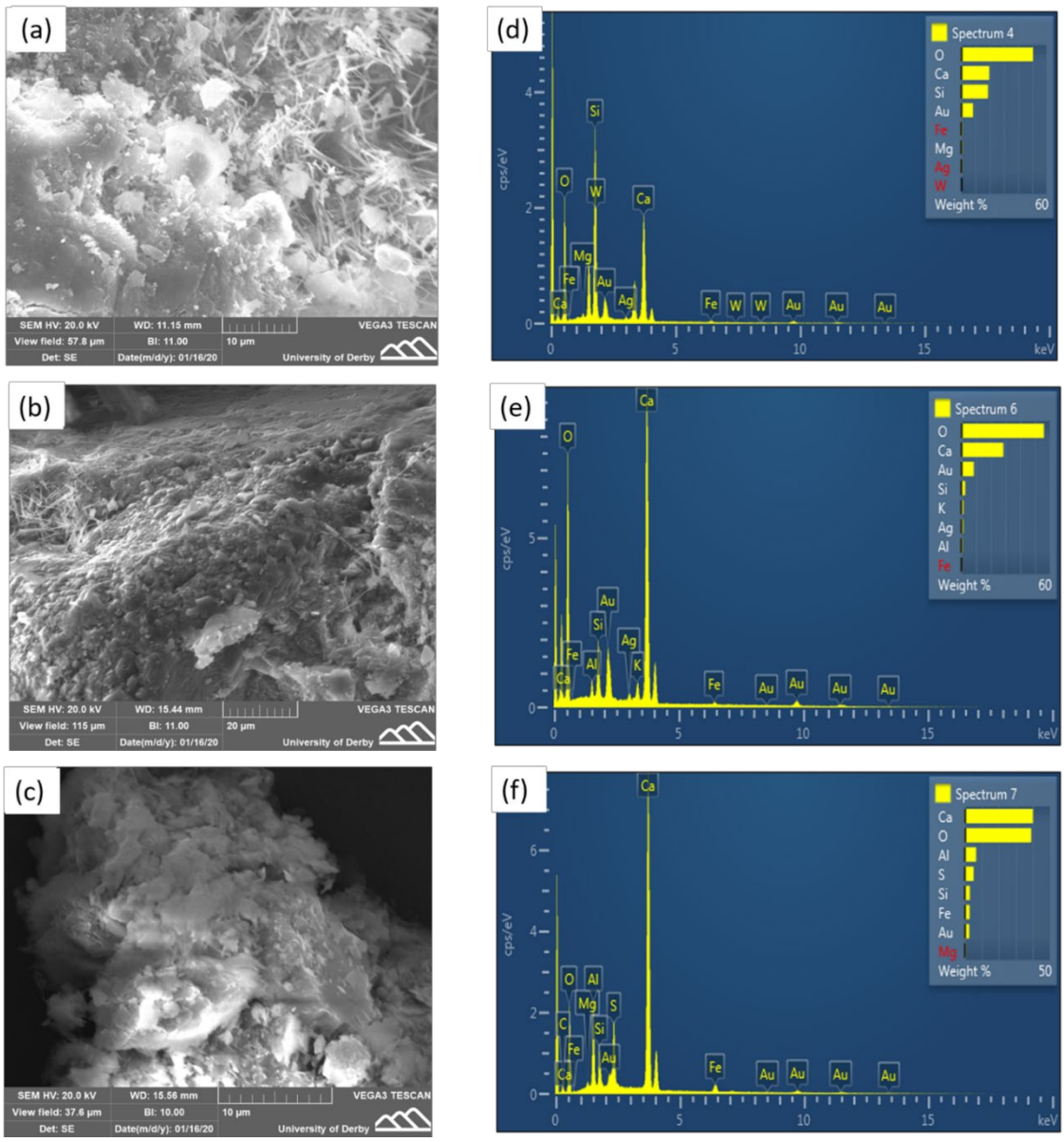

Fig. 8 (a, b, and c) SEM images of the healing products of the control mortar specimens CMS incubated in X0, XA1, and XA3, respectively. (d, e, and f) EDX analysis of the healing products of the control mortar specimens incubated in X0, XA1, and XA3, respectively

CONCLUSION

This study investigated the performance of bio-self-healing cementitious mortar in clay soil under different exposure conditions (pH, sulphate and water saturation). The quantification results of crack healing ratios using image analysis were consistent with water absorption testing.

According to the findings, it can be inferred that the bio-self-healing was more efficient for all exposure classes than the autogenous healing experienced by the control specimens. However, these efficiencies were significantly

affected by the soil's moisture content, where the healing performance of bio-mortar specimens incubated in fully saturated conditions was around 40% higher than in the partially saturated condition. This suggests that the mineral precipitation of calcium carbonate induced by bacterial metabolic conversion of nutrients is highly dependent on soil moisture content. The hydration of un-hydrated cement particles representing the primary source of autogenous healing is also influenced by soil moisture content.

Compared with the partially saturated condition, the healing ratios in the fully saturated condition were larger. This is because there was less pore water available to sustain bacterial activity. This suggests that bio-self-healing of concrete occurs in a similar way within the soil. Indeed, this has been shown to be the case for concrete incubated in humid air and water, with optimal results obtained in full water incubation.

The healing ratios of bio mortar specimens incubated in the clay soil with different levels of pH and sulphate (X0, XA1, and XA3) were almost similar, with better results observed in the pH-neutral condition. Therefore, it can be concluded that the effect of soil pH and sulphate on bio-self-healing is relatively small (in comparison with the effect of soil moisture content).

However, further research is required to determine whether these results were also influenced by a biological feature or other abiotic factors, such as the existence of a soil matrix that prevents oxygen and other resources from being transported to the microbes, impeding their ability to generate CO_2.

From a design perspective, this study shows that the bio-self-healing technique can generally benefit concrete structures embedded within clay soil under all conditions (adopted in the experiments). However, on the other hand, the study emphasises the need to consider the groundwater regime as well as the acidity and sulphate of the ground.

DATA AVAILABILITY STATEMENT

All data that support the findings of this study are available from the corresponding author upon reasonable request.

ACKNOWLEDGMENTS

We thank Graham Souch and Richard Duff for their technical assistance in this study.

SUPPLEMENTAL DATA

Figs. S1–S5 are available online in the ASCE Library (ascelibrary.org).

REFERENCES

Alazhari, M., T. Sharma, A. Heath, R. Cooper, and K. Paine. 2018. “Application of expanded perlite encapsulated bacteria and growth media for self-healing concrete.” *Constr. Build. Mater.*, 160: 610–619.

Alghamri, R., A. Kanellopoulos, and A. Al-Tabbaa. 2016. “Impregnation and encapsulation of lightweight aggregates for self-healing concrete.” *Constr. Build. Mater.*, 124: 910–921.

De Belie, N., E. Gruyaert, A. Al-Tabbaa, P. Antonaci, C. Baera, D. Bajare, A. Darquennes, R. Davies, L. Ferrara, T. Jefferson, C. Litina, B. Miljevic, A. Otlewska, J. Ranogajec, M. Roig-Flores, K. Paine, P. Lukowski, P. Serna, J.-M. Tulliani, S. Vucetic, J. Wang, and H. M. Jonkers. 2018. “A Review of Self-Healing Concrete for Damage Management of Structures.” *Adv. Mater. Interfaces*, 5 (17): 1800074. Wiley-VCH Verlag. https://doi.org/10.1002/admi.201800074.

BS EN. 2015. *BS EN 480-13:2015 Admixtures for concrete, mortar and grout. Test methods Reference masonry mortar for testing mortar admixtures*.

BSI. 1990a. *BS 1377-2:1990 Methods of test for soils for civil engineering purposes. Part 2: Classification tests*. London: British Standards Institution.

BSI. 1990b. *BS 1377-3:1990, Methods of test for soils for civil engineering purposes. Part 3: Chemical and electro-chemical tests*. London: British Standards Institution.

BSI. 2000. *BS EN 1097-6 Tests for mechanical and physical properties of aggregates - Part 6: Determination of particle density and water absorption*. *October*, 32. London: British Standards Institution.

BSI. 2004. *BS EN 13295:2004 Products and Systems for the Protection and Repair of Concrete Structures - Test methods - Determination of resistance to carbonation*. *Br. Stand. Instiution*, 1–18. London: British Standrds Institution.

BSI. 2016. *BS EN 206:2013+A1:2016. Concrete. specification, performance, production and conformity*. London: British Standrds Institution.

Cappuccino, J., and N. Sherman. 2018. *Microbiology: a laboratory manual*. Harlow, England: Pearson Education Limited.

Chen, H., C. Qian, and H. Huang. 2016. “Self-healing cementitious materials based on bacteria and nutrients immobilized respectively.” *Constr. Build. Mater.*, 126: 297–303.

Dry, C. 1994. “Matrix cracking repair and filling using active and passive modes for smart timed release of chemicals from fibers into cement matrices.” *Smart Mater. Struct.*, 3 (2): 118.

Edvardsen, C. 1999. “Water permeability and autogenous healing of cracks in concrete.” *Mater. J.*, 96 (4): 448–454.

Esaker, M., O. Hamza, A. Souid, and D. Elliott. 2021. “Self-healing of bio-cementitious mortar incubated within neutral and acidic soil.” *Mater. Struct. 2021 542*, 54 (2): 1–16. Springer. https://doi.org/10.1617/S11527-021-01690-1.

Gardner, D., A. Jefferson, A. Hoffman, and R. Lark. 2014. “Simulation of the capillary flow of an autonomic healing agent in discrete cracks in cementitious materials.” *Cem. Concr. Res.* Pergamon.

Gonzalez-Ollauri, A., and S. B. Mickovski. 2017. “Plant-soil reinforcement response under different soil hydrological regimes.” *Geoderma*, 285: 141–150. Elsevier B.V. https://doi.org/10.1016/j.geoderma.2016.10.002.

Gupta, S., H. W. Kua, and S. Dai Pang. 2018. “Healing cement mortar by immobilization of bacteria in biochar: An integrated approach of self-healing and carbon sequestration.” *Cem. Concr. Compos.*, 86: 238–254.

Hamza, O., and A. Bellis. 2008. “Gault Clay embankment slopes on the A14 - Case studies of shallow and deep instability.” *Adv. Transp. Geotech. - Proc. 1st Int. Conf. Transp. Geotech.*, 307–316. CRC Press.

Hamza, O., M. Esaker, D. Elliott, and A. Souid. 2020. “The effect of soil incubation on bio self-healing of cementitious mortar.” *Mater. Today Commun.*, 24: 100988. Elsevier Ltd. https://doi.org/10.1016/j.mtcomm.2020.100988.

Hamza, O., and J. Ikin. 2020. “Electrokinetic treatment of desiccated expansive clay.” *Géotechnique*, 70 (5): 421–431. ICE Publishing. https://doi.org/10.1680/jgeot.18.P.266.

Ter Heide, N. 2005. “Crack healing in hydrating concrete.” *Delft Univ. Technol.*

Imokawa, G., and M. Hattori. 1985. “A possible function of structural lipids in the water-holding properties of the stratum corneum.” *J. Invest. Dermatol.*, 84 (4): 282–284. Elsevier. https://doi.org/10.1111/1523-1747.ep12265365.

Institution, B. S. 2016. “BS EN 206:2013+A1:2016. Concrete — Specification, performance, production and conformity.” London.

Jonkers, H. M., and E. Schlangen. 2007. “Self-healing of cracked concrete: a bacterial approach.” *Proc. FRACOS6 Fract. Mech. Concr. Concr. Struct. Catania, Italy*, 1821–1826.

Kalhori, H., and R. Bagherpour. 2017. “Application of carbonate precipitating bacteria for improving properties and repairing cracks of shotcrete.” *Constr. Build. Mater.*, 148: 249–260. Elsevier Ltd.

https://doi.org/10.1016/j.conbuildmat.2017.05.074.

Knoll, A. H. 2003. “Biomineralization and Evolutionary History.” *Rev. Mineral. Geochemistry*, 54 (1): 329–356. GeoScienceWorld. https://doi.org/10.2113/0540329.

Lee, Y. S., and W. Park. 2018. “Current challenges and future directions for bacterial self-healing concrete.” *Appl. Microbiol. Biotechnol.* Springer Verlag.

Martys, N. S., and C. F. Ferraris. 1997. “Capillary transport in mortars and concrete.” *Cem. Concr. Res.*, 27 (5): 747–760. Elsevier Ltd. https://doi.org/10.1016/S0008-8846(97)00052-5.

Mors, R., and H. M. Jonkers. 2020. “Bacteria-based self-healing concrete: evaluation of full scale demonstrator projects.” *RILEM Tech. Lett.*, 4: 138–144. Rilem Publications SARL. https://doi.org/10.21809/rilemtechlett.2019.93.

Palin, D., V. Wiktor, and H. M. Jonkers. 2017. “A bacteria-based self-healing cementitious composite for application in low-temperature marine environments.” *Biomimetics*, 2 (3): 13.

Pei, R., J. Liu, S. Wang, and M. Yang. 2013. “Use of bacterial cell walls to improve the mechanical performance of concrete.” *Cem. Concr. Compos.*, 39: 122–130. Elsevier Ltd. https://doi.org/10.1016/j.cemconcomp.2013.03.024.

Perito, B., and G. Mastromei. 2011. “Molecular basis of bacterial calcium carbonate precipitation.” *Prog. Mol. Subcell. Biol.*, 52: 113–139. Springer, Berlin, Heidelberg. https://doi.org/10.1007/978-3-642-21230-7_5.

Schlangen, E., and S. Sangadji. 2013. “Addressing infrastructure durability and sustainability by self healing mechanisms-recent advances in self healing concrete and asphalt.” *Procedia Eng.*, 54: 39–57.

Schneider, C. A., W. S. Rasband, and K. W. Eliceiri. 2012. “NIH Image to ImageJ: 25 years of image analysis.” *Nat. Methods 2012 97*, 9 (7): 671–675. Nature Publishing Group. https://doi.org/10.1038/nmeth.2089.

Sonenshein, A. L., B. Cami, J. Brevet, and R. Cote. 1974. “Isolation and characterization of rifampin-resistant and streptolydigin-resistant mutants of Bacillus subtilis with altered sporulation properties.” *J. Bacteriol.*, 120 (1): 253–265.

Souid, A., M. Esaker, D. Elliott, and O. Hamza. 2019. “Experimental data of bio self-healing concrete incubated in saturated natural soil.” *Data Br.* Elsevier Inc.

Talaiekhozan, A., A. Keyvanfar, A. Shafaghat, R. Andalib, M. Z. A. Majid, M. A. Fulazzaky, R. M. Zin, C. T. Lee, M. W. Hussin, and N. Hamzah. 2014. “A review of self-healing concrete research development.” *J. Environ. Treat. Tech.*, 2 (1): 1–11.

Thomas, A. D., A. J. Dougill, D. R. Elliott, and H. Mairs. 2014. “Seasonal differences in soil CO2 efflux and carbon storage in Ntwetwe Pan, Makgadikgadi Basin, Botswana.” *Geoderma*, 219–220: 72–81. Elsevier. https://doi.org/10.1016/j.geoderma.2013.12.028.

Van Tittelboom, K., and N. De Belie. 2013. “Self-healing in cementitious materials—A review.” *Materials (Basel).*, 6 (6): 2182–2217.

Van Tittelboom, K., N. De Belie, W. De Muynck, and W. Verstraete. 2010. “Use of bacteria to repair cracks in concrete.” *Cem. Concr. Res.*, 40 (1): 157–166.

Tziviloglou, E., Z. Pan, H. M. Jonkers, and E. Schlangen. 2017. “Bio-based self-healing mortar: An experimental and numerical study.” *J. Adv. Concr. Technol.*, 15 (9): 536–543.

Wang, J., K. Van Tittelboom, N. De Belie, and W. Verstraete. 2012. “Use of silica gel or polyurethane immobilized bacteria for self-healing concrete.” *Constr. Build. Mater.*, 26 (1): 532–540.

Xu, J., W. Yao, and Z. Jiang. 2013. “Non-ureolytic bacterial carbonate precipitation as a surface treatment strategy on cementitious materials.” *J. Mater. Civ. Eng.*, 26 (5): 983–991.

Yang, Y., E.-H. Yang, and V. C. Li. 2011. “Autogenous healing of engineered cementitious composites at early age.” *Cem. Concr. Res.*, 41 (2): 176–183.

Zhang, J., Y. Liu, T. Feng, M. Zhou, L. Zhao, A. Zhou, and Z. Li. 2017. “Immobilizing bacteria in expanded perlite for the crack self-healing in concrete.” *Constr. Build. Mater.*, 148: 610–617.

van der Zwaag, S. 2007. “An introduction to material design principles: Damage prevention versus damage management.” *Self Heal. Mater.*, 1–18. Springer.